



OPEN ACCESS

EDITED BY

Zhongyang Luo,
Zhejiang University, China

REVIEWED BY

Gianluigi De Falco,
DICMAPI—University of Naples Federico
II, Italy
Patrick Mountapbeme Kouotou,
National Advanced School of
Engineering of Maroua/ Researcher,
Cameroon

*CORRESPONDENCE

Yaoyao Ying,
yingyaoyao@njjust.edu.cn
Dong Liu,
dongliu@njjust.edu.cn

SPECIALTY SECTION

This article was submitted to Advanced
Clean Fuel Technologies,
a section of the journal
Frontiers in Energy Research

RECEIVED 30 June 2022

ACCEPTED 20 July 2022

PUBLISHED 11 August 2022

CITATION

Ying Y, Duan J and Liu D (2022), Effects
of the upward-increasing gradient
magnetic field on soot properties in
ethylene inverse diffusion flames with
different oxygen concentrations.
Front. Energy Res. 10:982391.
doi: 10.3389/fenrg.2022.982391

COPYRIGHT

© 2022 Ying, Duan and Liu. This is an
open-access article distributed under
the terms of the [Creative Commons
Attribution License \(CC BY\)](https://creativecommons.org/licenses/by/4.0/). The use,
distribution or reproduction in other
forums is permitted, provided the
original author(s) and the copyright
owner(s) are credited and that the
original publication in this journal is
cited, in accordance with accepted
academic practice. No use, distribution
or reproduction is permitted which does
not comply with these terms.

Effects of the upward-increasing gradient magnetic field on soot properties in ethylene inverse diffusion flames with different oxygen concentrations

Yaoyao Ying^{1,2*}, Jiaqi Duan^{1,2} and Dong Liu^{1,2*}

¹MIIT Key Laboratory of Thermal Control of Electronic Equipment, School of Energy and Power Engineering, Nanjing University of Science and Technology, Nanjing, China, ²Advanced Combustion Laboratory, School of Energy and Power Engineering, Nanjing University of Science and Technology, Nanjing, China

The effects of the upward-increasing gradient magnetic field on soot properties are experimentally investigated in ethylene inverse diffusion flames with different oxygen concentrations. The soot morphology, nanostructure, graphitization degree, and oxidation reactivity are obtained by high-resolution transmission electron spectroscopy (HRTEM), X-ray diffractometer (XRD), and thermogravimetric analyzer (TGA), respectively. The upward-increasing gradient magnetic field is induced by two Nd-Fe-B permanent magnets with different thicknesses. The results show that the magnetic field influences the soot properties mainly by affecting the distributions of paramagnetic O₂ and OH radicals in the flames. The soot samples are more graphitized in the flame with higher O₂ concentration, which contains a longer fringe length and smaller fringe tortuosity. Fullerene-like structures are more apparent with increasing oxygen content. The soot fringe length decreases and fringe tortuosity increases when the upward-increasing gradient magnetic field is applied. The application of the magnetic field enhances the soot oxidation reactivity, and it shows the greatest effect on the oxidation reactivity of soot produced in the flame with 21% O₂ content.

KEYWORDS

soot properties, magnetic field, inverse diffusion flame, nanostructure, oxidation reactivity

Introduction

With the rapid growth of the world's population and industrialization, global energy demand continues to grow in the coming decades. Large-scale development and use of fossil energy will do great harm to the climate and environment. In addition to greenhouse gases, there are hazardous pollutants such as nitrogen oxides, unburned hydrocarbons, soot, etc., (Wang and Chung, 2019; Li et al., 2021; Falco et al., 2022). Soot, emitted from the pyrolysis and incomplete burning of hydrocarbon fuels, may

cause cardiac arrest, asthma, and pulmonary diseases (Arif et al., 2018; Ali et al., 2021). Recent studies have shown that the transmission rate and incidence of novel coronavirus pneumonia (COVID-19) are closely related to local atmospheric particulate matter concentration (Mehmood et al., 2020; Chakrabarty et al., 2021).

The physical factors affecting soot formation mainly include temperature, pressure, magnetic field, etc. A detailed study of the physical parameters contributes to a better design of the burner structure and reduces the generation and emission of soot. The utilization of a magnetic field is one of the potential strategies for combustion control (Agarwal et al., 2014; Agarwal et al., 2015). The magnetic field can affect the flame temperature, flame structure, and free radical distribution, which has been widely studied (Takashi, 1990; Gilard et al., 2008). During the combustion process, charged ions or ion clusters are generated, and the applied magnetic field produces the Lorentz force, which changes the direction of motion of the charged particles, thereby affecting the chemical reaction rate caused by the concentration change. In addition to the Lorentz force for ionic species, the non-conductive and paramagnetic substances are subjected to the magnetic force, which contributes to a significant effect on chemical reactions in flames (Shinoda, 2005).

In recent years, researchers have conducted studies on the change of gradient magnetic field on the combustion characteristics of gas fuel. The magnetic force increases the concentration of OH radicals toward the flame center, which is attributed to the effect of the magnetic field on paramagnetic O₂ (Yamada et al., 2002; Yamada et al., 2003a). The paramagnetic force does not directly affect OH radicals, instead, the paramagnetic force acts on O₂ with higher magnetic susceptibility and density, leading to the convective motion of O₂ and changing the distribution of OH radicals. The combustion characteristics of butane diffusion flames are investigated under different kinds of magnetic fields, and it is observed that the flame temperature increases in an upward-decreasing gradient of magnetic field and decreases with an upward-increasing magnetic field gradient (Aoki, 1990; Kumar et al., 2015). Experimental investigations are conducted to assess the effects of the gradient of the square of the magnetic flux density ($\nabla(B^2)$) on the sooting tendency in non-premixed flames (Jocher et al., 2015) and partially premixed flames (Jocher et al., 2017). In non-premixed flames, increasing the magnetic gradient promotes soot production, while the upward ($\nabla(B^2)$) contributes to a reduction of soot for some partially premixed flames. Moreover, the magnetic field enhances the soot production by extending the residence time in flames with different oxidizer mixtures and increases the heat radiation of soot (Jocher et al., 2019).

It can be found that the application of a gradient magnetic field can affect the flame temperature, flame structure, free radical distributions, and sooting tendency. The influence of magnetic field on flame characteristics has been studied, but the effects of gradient magnetic field on the soot properties needs

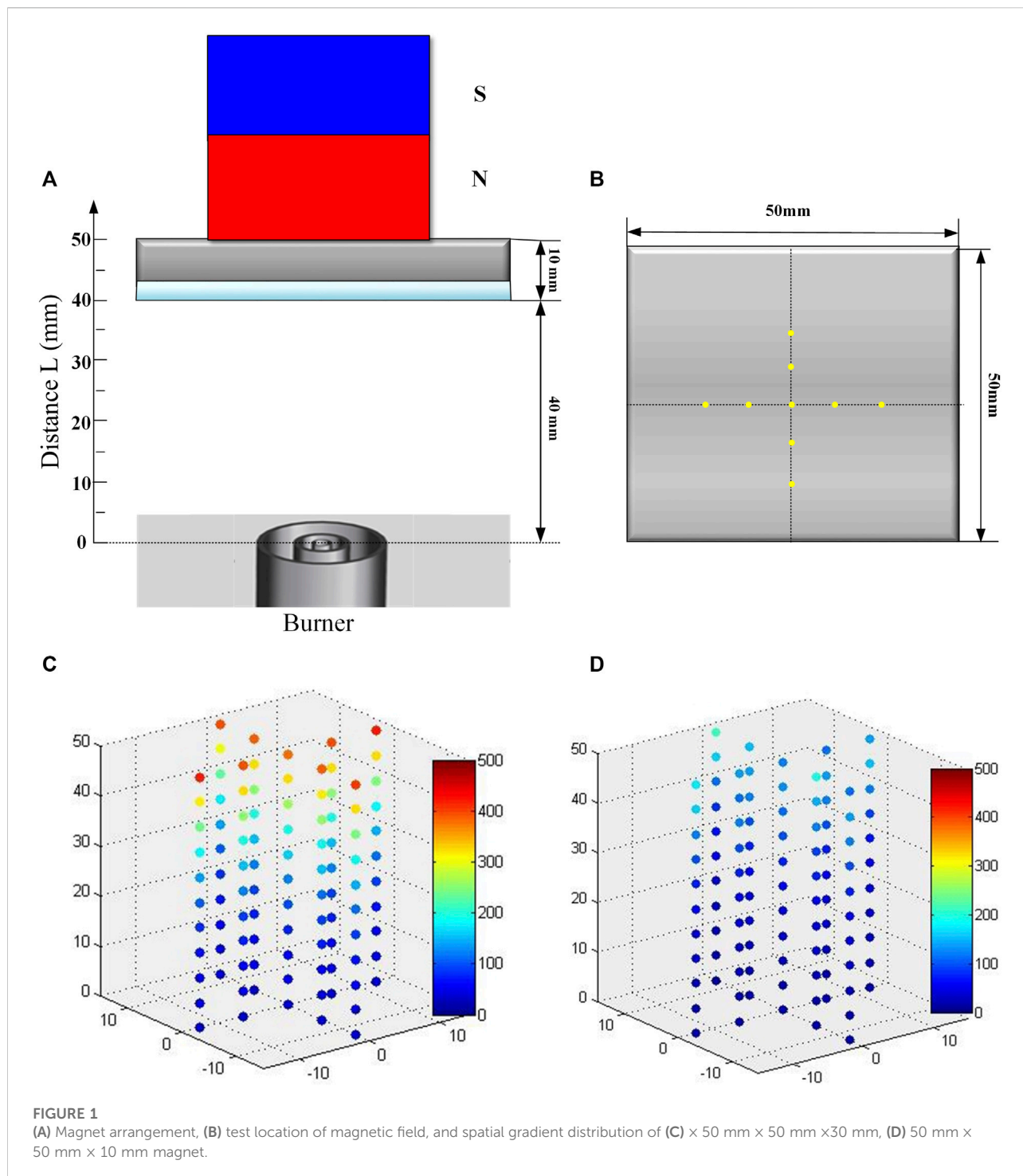
further investigation. This study aims to analyze the effects of the upward-increasing gradient magnetic field on soot properties in inverse diffusion ethylene flames with different oxygen concentrations. The soot properties including morphology, nanostructure, graphitization degree, and oxidation activity of the soot are obtained by high-resolution transmission electron spectroscopy (HRTEM), X-ray diffractometer (XRD), and thermogravimetric analyzer (TGA), respectively.

Experimental

An inverse diffusion flame burner is used in this study as in the previous work (Ying and Liu, 2017; Ying and Liu, 2021). The upward-increasing gradient magnetic field is induced by two Nd-Fe-B permanent magnets with different thicknesses, where the specific dimensions are $\times 50 \text{ mm} \times 50 \text{ mm} \times 10 \text{ mm}$ and $50 \text{ mm} \times 50 \text{ mm} \times 30 \text{ mm}$. The Nd-Fe-B permanent magnet is placed above the cooling plate as Figure 1A shows. The quartz glass plate under the cooling plate is 40 mm away from the burner outlet. The magnetic field distributions of the two magnets are measured by taking the center of the magnet as the base point and arranging a measurement point every 6.25 mm along with the horizontal and vertical directions. The yellow circles in Figure 1B present the test positions. The magnetic field distribution is measured along the burner axis in units of 5 mm to ensure that the measurement area can completely cover the flame. The magnetic field gradient increases with the increasing height along the flame axis. For the magnet with a size of $\times 50 \text{ mm} \times 50 \text{ mm} \times 30 \text{ mm}$, the average magnetic field strength at 40 mm from the burner is 248.67 and 37.65 mT at the burner surface. While for the magnet with a size of $\times 50 \text{ mm} \times 50 \text{ mm} \times 10 \text{ mm}$, the average magnetic field strength at the same positions is 119.07 and 16.78 mT, respectively. The detailed magnetic field gradient distributions are shown in Figures 1C,D.

The gas molecules and activated groups in the flame can be divided into paramagnetic substances and diamagnetic substances, especially the two substances O₂ and OH radicals. The ratio of O₂ on the oxidative side is set to 21, 26, and 31% to study the effect of oxygen concentration on soot formation under a magnetic field. The flames with three different oxygen concentrations are abbreviated as F1, F2, and F3, respectively, and the following numbers indicate the thickness of the permanent magnet. The detailed flame conditions are shown in Table 1.

The soot is collected by quartz plate sampling method in the post-flame area at HAB = 40 mm for 15 min. The soot mass is weighted for each condition at least three times. The characterization methods and settings are the same as the previous studies (Ying et al., 2017; Ying and Liu, 2018).



Briefly, the soot morphology and nanostructure are observed by a Tecnai G2 F30 HRTEM. To obtain the soot fringe characteristic parameters, a homemade MATLAB procedure is used (Ying and Liu, 2017). A Bruker D8 Advance XRD is applied to assess the graphitization degree of soot, and the soot oxidation reactivity is tested by a Netzsch STA449 F3 Jupiter TGA.

Results and discussion

O₂ concentration distribution

The magnetically induced variation in the spatial distribution of paramagnetic O₂ is measured at 21% oxygen content as a

TABLE 1 The detailed flame conditions.

Flame notation	Magnetic field (mm)	Oxidizer (mol%)	Gas flow rate (l/min)			
			C ₂ H ₄	N ₂ (dilution)	Oxidizer	N ₂ (shield)
F1-0	—	21% O ₂ +79% N ₂	0.7	0.7	0.7	13
F1-10	50 × 50 × 10					
F1-30	50 × 50 × 30					
F2-0	—	26% O ₂ +74% N ₂				
F2-10	50 × 50 × 10					
F2-30	50 × 50 × 30					
F3-0	—	31% O ₂ +69% N ₂				
F3-10	50 × 50 × 10					
F3-30	50 × 50 × 30					

TABLE 2 Soot mass collected by quartz plate (Unit: mg).

O ₂ ratio	21%	26%	31%
Magnet (mm)			
—	9.2 ± 0.4	19.6 ± 0.6	26.8 ± 1.2
50 × 50×10	10.6 ± 1.2	22.5 ± 0.9	27.4 ± 2.2
50 × 50×30	10.7 ± 0.6	23.6 ± 2.4	29.5 ± 3.1

representative. The gas is assessed on the centerline and boundary of the flame at the height above the burner HAB = 15, 25, and 35 mm by an online detection system. The O₂ concentration increases along with the flame centerline with the upward-increasing gradient magnetic field, especially at HAB = 15 mm, the oxygen content is significantly higher than that of the flame without the magnetic field. The gradient magnetic field causes the O₂ concentration to drop significantly along the flame boundary. The change in O₂ concentration along the flame centerline and boundary at different flame conditions are shown in [Supplementary Figure S1](#). It is found that in the upward-increasing gradient magnetic field, O₂ moves toward the flame center due to its paramagnetic susceptibility. Therefore, it can be inferred that paramagnetic OH radicals also shift to the flame center with the magnetic field.

Soot mass

[Table 2](#) lists the soot mass in the flames collected by the quartz plate at HAB = 40 mm. The flame with a 21% O₂ concentration and no magnetic field has the lowest soot production of 9.2 mg, while the flame with an oxygen concentration of 31% under the influence of a strong magnetic field produces the highest soot mass, 29.5 mg. It is

found that increasing the oxygen concentration leads to increased soot formation. Under the same O₂ concentration conditions, the soot mass also increases with the increasing magnetic field. This may be because the fuel generates charged particles during the pyrolysis process and is in the form of ions or ion clusters. When a certain magnetic field is applied, these ions or ion clusters are affected by the Lorentz force and changed from the original disordered Brownian diffusion motion to an ordered upward motion ([Yamada et al., 2003b](#)). As a result, the enhanced combustion increases the maximum flame temperature and promotes soot formation. After HAB = 10 mm, the soot mass increase is dominated by the agglomeration between soot particles.

Soot morphology

[Figure 2](#) shows the typical TEM images of soot under different flame conditions. The soot particles generated by the ethylene inverse diffusion flame with a 21% O₂ concentration have irregular liquid-like protrusions, which are mainly caused by the condensation of soot precursors like polycyclic aromatic hydrocarbons (PAHs) on the surface of solid particles ([Alfè et al., 2009](#)). When the upward-increasing gradient magnetic field is applied, the liquid-like substance increases and the protrusions transform into a sheet-like structure. The particle size of the soot decreases without an external magnetic field when the oxygen content increases to 26%. The particles cluster highly together and individual particles are difficult to distinguish from one another. The solid properties of the particles are more evident than those with low oxygen content. For F2-10 and F2-30 conditions, the clustered soot is wrapped in liquid-like material, and the larger coverage area of the liquid material can be observed with the larger magnetic field.

When the oxygen ratio is 31%, the agglomerated soot particles contain an increased number of primary soot

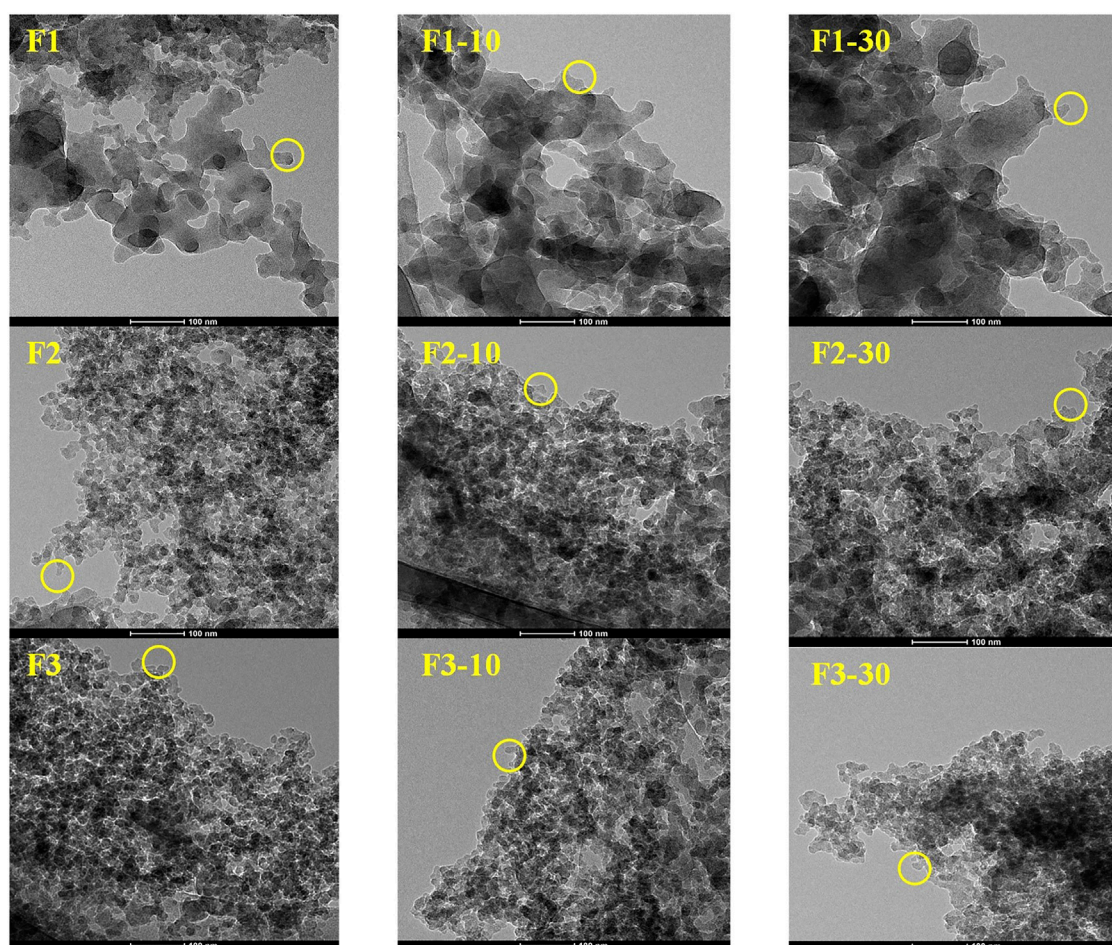


FIGURE 2
Typical TEM images of soot in flames with different magnetic fields.

particles compared to low oxygen concentrations. After adding an upward-increasing gradient magnetic field, the morphology is still a cluster of hundreds or thousands of nearly spherical elementary particles, but the particle edges are slightly blurred. From the above TEM images, it can be found that with increasing oxygen concentration, the content of liquid-like substances decreases and the agglomeration degree increases. When an upward-increasing gradient magnetic field is applied, the surface of the particles grows slowly due to the low flame temperature in the primary region. Moreover, collisions and condensation occur between the particles, and the PAHs covered on the surface increase.

Soot nanostructure

To further obtain the nanostructure of the soot, the yellow circle areas shown in [Figure 2](#) are magnified by HRTEM. [Figure 3](#)

presents the typical HRTEM images of soot. Those with long, straight, ordered, and regularly arranged fringes represent a higher degree of carbonization, while the curved, disordered, and randomly distributed fringes stand for a lower degree of maturity ([Ying and Liu, 2017](#)). The soot particles in the F1 flame show a disordered structure, in which no clear center is found and the direction of the fringes is random. The degree of the fringe disorder increases with the increasing magnetic field.

For the soot in the F2 flame, the arrangement of the inner fringes becomes more ordered, and different-sized outer shells are formed, which shows a typical fullerene-like structure. This is mainly because the total flame temperature increases with increasing oxygen ratio. The oxidation reaction causes the PAH layers stacked on the particle surface to be oxidized and aggregate several particles to form new condensed soot particles. However, for F2-10 and F2-30 conditions, the inner part also exhibits a fullerene-like structure consisting of partially curved fringes, but the outer shells are relatively disordered. This

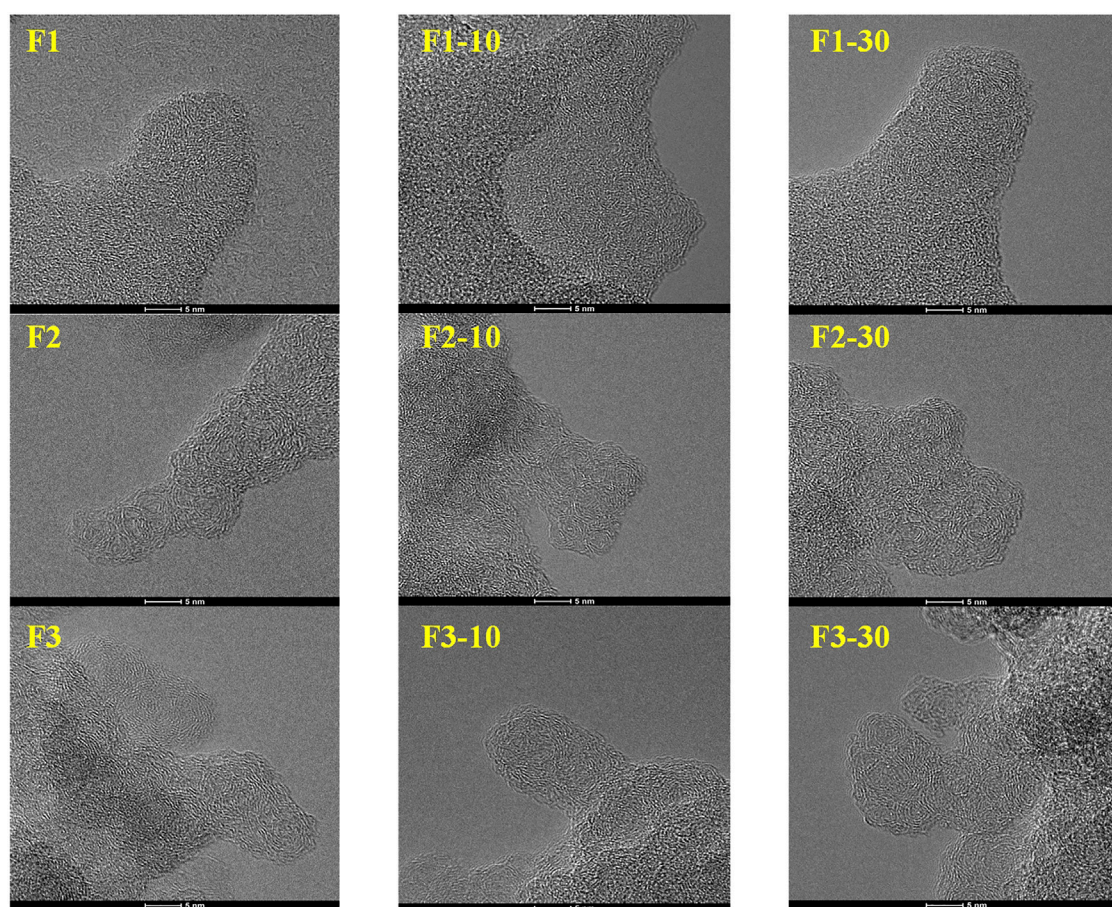


FIGURE 3
Typical HRTEM images of soot in flames with different magnetic fields.

variation is mainly because the paramagnetic force acting on the O_2 and OH radicals changes their movements after the application of an upward-increasing gradient magnetic field. While the oxidant side of the inverse diffusion burner is located in the center, the oxygen diffusion to the fuel side becomes poor. Therefore, the surface growth rate of the soot is slowed down and the degree of carbonization is relatively low. Compared with the soot in the F2 flame, the fullerene-like nanostructure of the soot particles in the F3 flame is more obvious and frequent. The center is more defined and the outer shell is composed of longer and more ordered fringes. This is because the soot particles grow faster in the high-temperature reaction region with 31% O_2 content and the fringes are relatively long and straight. However, even when an external magnetic field is applied, the nanostructure observed by the naked eye is not significantly changed.

To further compare the differences in the soot nanostructure quantitatively, the skeletonized images of the typical HRTEM images are shown in Figure 4. The extracted

fringe length and tortuosity are calculated and the average values are listed in Table 3. The detailed distribution of fringe length and tortuosity and mean value of soot particles under different flame conditions are presented in Supplementary Figure S2. For the F1 flame, the average fringe length is 0.93 nm, and 61% of the fringes are less than 1 nm. When an upward-increasing gradient magnetic field is arranged, the mean fringe length decreases with the increasing magnetic field, and the minimum average fringe length is 0.91 nm for F1-30 soot. The average fringe length of the soot produced by the flame with 26% oxygen concentration is longer and the fringes are mainly concentrated in the range of 0.8–1.0 nm. In the magnetic field flame, the fringe length decreases slightly and is mainly distributed between 0.7 and 0.9 nm. The mean fringe length of the soot reaches the maximum value of 1.01 nm in flame with 31% oxygen content. The fringe distribution range is wide, with 47.6% fringes longer than 1 nm. With the increasing magnetic field, the average fringe length decreases at the same oxygen content,

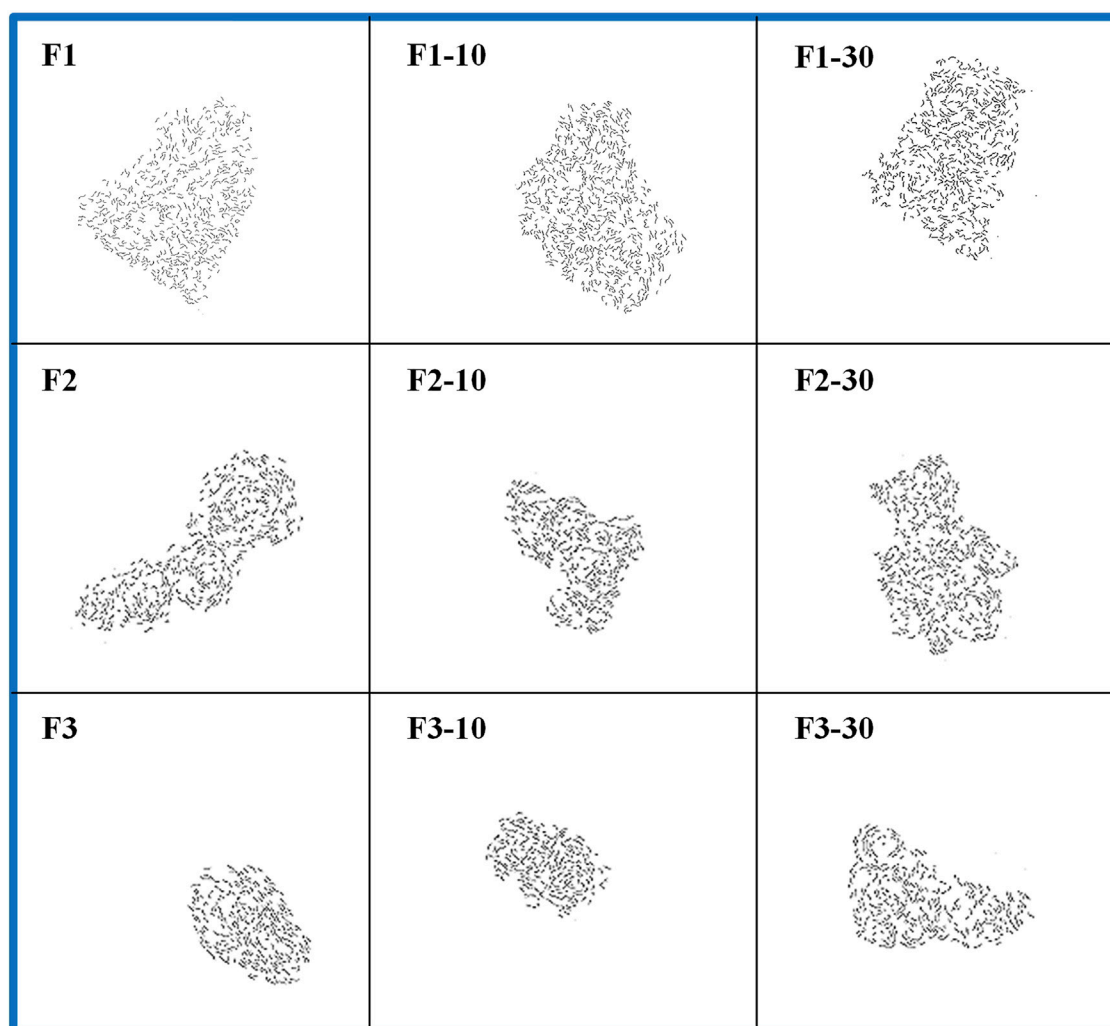


FIGURE 4
Skeletonized output images of the typical HRTEM images.

TABLE 3 Mean fringe length and tortuosity with standard deviations of the soot.

Flame	Fringe length (nm)	Fringe tortuosity
F1-0	0.93 ± 0.02	1.37 ± 0.01
F1-10	0.92 ± 0.05	1.38 ± 0.02
F1-30	0.91 ± 0.04	1.38 ± 0.01
F2-0	0.99 ± 0.08	1.26 ± 0.02
F2-10	0.96 ± 0.03	1.27 ± 0.03
F2-30	0.95 ± 0.04	1.28 ± 0.02
F3-0	1.01 ± 0.04	1.20 ± 0.03
F3-10	0.99 ± 0.04	1.23 ± 0.01
F3-30	0.97 ± 0.05	1.24 ± 0.02

and the shortest fringe length is 0.97 nm for the soot in the F3-30 flame. In an environment with sufficient oxygen, the fringes are susceptible to oxidation and the arrangement is more regular, so the average fringe length increases. However, with an upward-increasing gradient magnetic field, the paramagnetic force inhibits the diffusion and convection movement of O_2 to the flame side (Yamada et al., 2003), thus retarding the nucleation and surface growth of soot particles. The lower degree of carbonization further influence the fringe arrangement and length.

The change of fringe tortuosity is exactly opposite to the fringe length. The average value of the fringe tortuosity is $F1 < F1-10 < F1-30$ in the order from small to large with 21% O_2 concentration. The stacking sequence of the fringes is disordered as shown in Figure 4. The fringes are short and

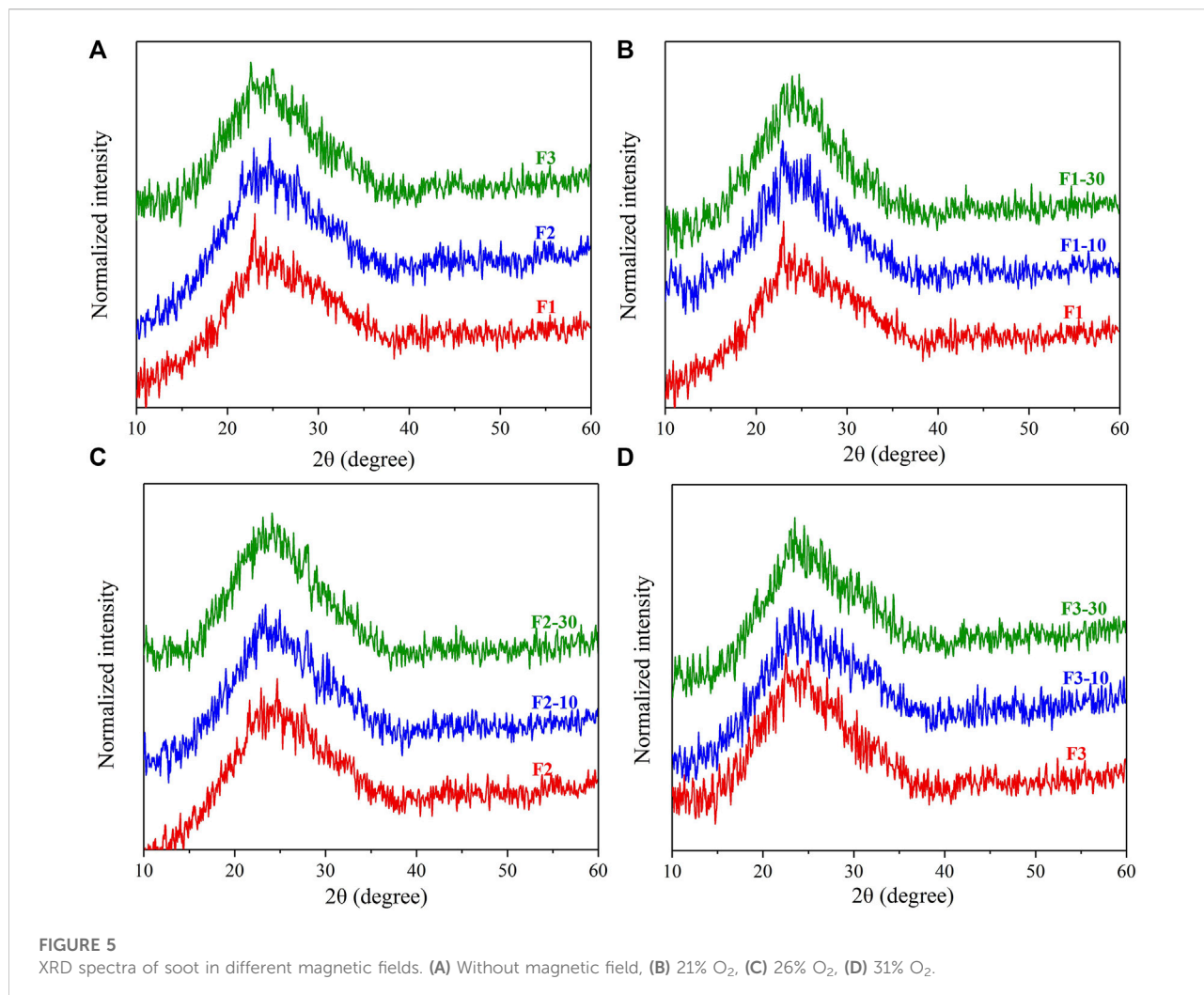


TABLE 4 Peak diffraction values of θ_{002} of the soot.

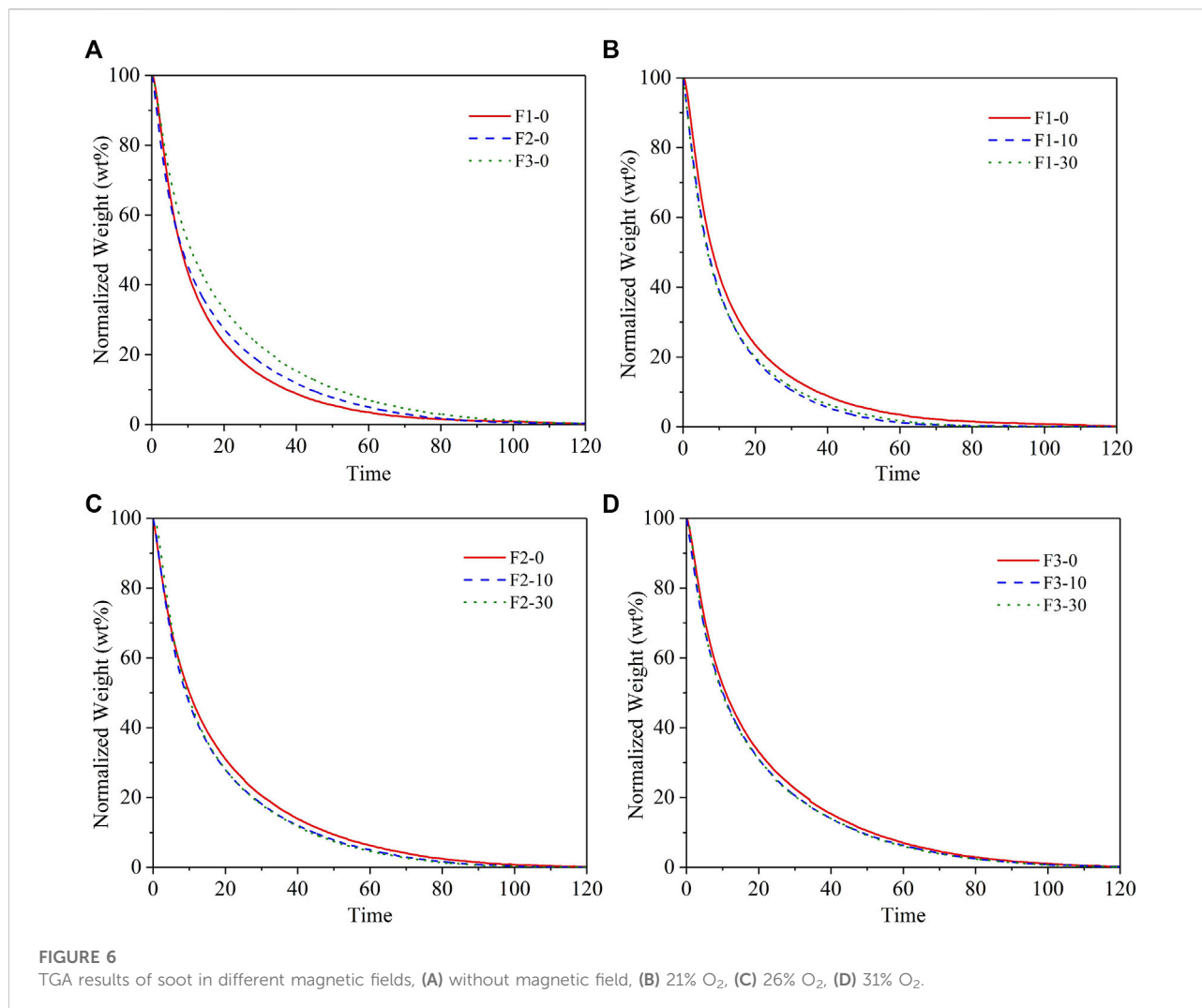
O ₂ ratio	21%	26%	31%
Magnet (mm)			
—	24.2683	24.6717	24.8733
50 × 50 × 10	24.1171	24.5204	24.7221
50 × 50 × 30	23.9658	24.3692	24.5708

curved. When 26% O₂ is added, the mean fringe tortuosity decreases, and the average fringe curvatures corresponding to the conditions of F2, F2-10, and F2-30 are 1.26, 1.27, and 1.28, respectively. The fringe tortuosity of soot particles without a magnetic field at 31% oxygen concentration is the smallest, 1.20. The fringe tortuosity increases slightly with the upward-increasing gradient magnetic field. It is evident that the fringe

length is negatively correlated with the fringe tortuosity: the longer the fringe length, the smaller the tortuosity.

Soot graphitization degree

Table 4 gives the (002) peak diffraction value of the soot. The soot all shows broadened diffraction peaks near 24° as the XRD spectra are shown in Figure 5. Since XRD is more sensitive to crystalline substances, it shows that all samples belong to an amorphous structure. The closer the diffraction angle of the (002) peak near 25°, the higher the degree of graphitization of soot particles. Combined with the offset of the (002) peak in Table 4, the peak position approaches 25° as the oxygen concentration increases, indicating that the graphitization degree of soot particles is enhanced and relatively more mature. At the same O₂ ratio, when the upward-increasing gradient magnetic field increases, the overall peak position shifts to the smaller side. The results show that the effect of the magnetic field significantly



reduces the graphitization degree of soot, which is consistent with the results of nanostructure analysis.

Soot oxidation reactivity

Figure 6 shows the weight loss curves of the soot at a constant temperature of 500 °C. The greater the slope of the curve, the faster the oxidation rate. As O₂ concentration increases in the flames, the oxidation rate of the soot gradually slows down shown in Figure 4A. Considering the weight loss curves in Figure 4B, the time required for soot generated in flames F1, F1-10, and F1-30 to consume 90% of their mass is 37.32, 32.30, and 30.82 min, respectively. The oxidation reactivity of soot is enhanced by the application of the upward-increasing gradient magnetic field. When the O₂ ratio increases to 26 and 31%, the effects of the magnetic field on the oxidation reactivity of soot are relatively weakened. The

time required for the soot produced in F3, F3-10, and F3-30 flames to oxidize to 90% of their mass is 51.34, 48.5, and 47.9 min, respectively.

The oxidation results show that the higher the proportion of O₂ added to the flames, the greater the influence in reactivity to the soot. When an upward-increasing gradient magnetic field is applied, the oxidation reactivity of soot is significantly enhanced at 21% O₂ content, whereas the effect of the magnetic field is relatively weak when the O₂ concentration is increased to 31%. This is because, at 21% O₂ content, the effects of the magnetic field have a greater influence on the direction of movement of O₂ and OH radicals, which lowers the flame temperature and inhibits nucleation and surface growth of soot. Therefore, the soot is nascent with the magnetic field, resulting in a low graphitization degree and high oxidation reactivity. When the O₂ concentration continues to increase to 31%, the ability to diffuse is strong due to the high O₂ content in the flame center, and the paramagnetic force generated by the magnetic field is relatively weak. The combined effects cause a slight change in soot reactivity.

Conclusion

This study investigates the effects of the upward-increasing gradient magnetic field on the soot properties in the ethylene inverse diffusion flames with different oxygen concentrations, including soot morphology, nanostructure, graphitization degree, and oxidation reactivity experimentally. The main results are summarized as follows:

- 1) The graphitization degree of soot with larger O₂ content is higher. The soot shows an amorphous carbon structure at 21% O₂ concentration, while fullerene-like structures appear with increasing oxygen content. The soot fringe length decreases and the fringe tortuosity increases with the upward-increasing gradient magnetic field.
- 2) The magnetic field has the greatest effect on the oxidation reactivity of soot produced in the flame with 21% O₂ concentration, and the oxidation rate is significantly accelerated. The effect of the magnetic field is relatively weak for the soot from the flame with 31% O₂ content.
- 3) The upward-increasing gradient magnetic field influences the flame structures mainly by affecting the movement of the paramagnetic O₂ and OH radicals, which subsequently changes the soot properties.

Data availability statement

The raw data supporting the conclusions of this article will be made available by the authors, without undue reservation.

Author contributions

YY: conceptualization, methodology, investigation, formal analysis; writing-original draft and editing, and

References

- Agarwal, S., Kumar, M., and Shakher, C. (2015). Experimental investigation of the effect of magnetic field on temperature and temperature profile of diffusion flame using circular grating talbot interferometer. *Opt. Lasers Eng.* 68, 214–221. doi:10.1016/j.optlaseng.2015.01.004
- Agarwal, S., Kumar, M., and Shakher, C. (2014). Temperature measurement of axisymmetric flames under the influence of magnetic field using talbot interferometry. *AIP Conf. Proc.* 1620, 485–491.
- Alfê, M., Apicella, B., Barbella, R., Rouzaud, J. N., Tregrossi, A., and Ciajolo, A. (2009). Structure–property relationship in nanostructures of young and mature soot in premixed flames. *Proc. Combust. Inst.* 32, 697–704. doi:10.1016/j.proci.2008.06.193
- Ali, M. U., Siyi, L., Yousaf, B., Abbas, Q., Hameed, R., Zheng, C., et al. (2021). Emission sources and full spectrum of health impacts of black carbon associated polycyclic aromatic hydrocarbons (PAHs) in urban environment: A review. *Crit. Rev. Environ. Sci. Technol.* 51, 857–896. doi:10.1080/10643389.2020.1738854
- Aoki, T. (1990). Radical emissions and anomalous reverse flames appearing in upward-increasing magnetic fields. *Jpn. J. Appl. Phys.* 29, 181–190. doi:10.1143/jjap.29.181
- Arif, M., Kumar, R., Kumar, R., Eric, Z., and Gourav, P. (2018). Ambient black carbon, PM_{2.5} and PM₁₀ at patna: Influence of anthropogenic emissions and brick kilns. *Sci. Total Environ.* 624, 1387–1400. doi:10.1016/j.scitotenv.2017.12.227
- Chakrabarty, R. K., Beeler, P., Liu, P., Goswami, S., Harvey, R. D., Pervez, S., et al. (2021). Ambient PM_{2.5} exposure and rapid spread of COVID-19 in the United States. *Sci. Total Environ.* 760, 143391. doi:10.1016/j.scitotenv.2020.143391
- Falco, G. De., Bocchicchio, S., Commodo, M., Minutolo, P., and D'Anna, A. (2022). Raman spectroscopy of nascent soot oxidation: Structural analysis during heating. *Front. Energy Res.* 10, 878171. doi:10.3389/fenrg.2022.878171
- Gilard, V., Gillon, P., Blanchard, J.-N., and Sarh, B. (2008). Influence of A Horizontal magnetic field on A Co-flow methane/air diffusion flame. *Combust. Sci. Technol.* 180, 1920–1935. doi:10.1080/00102200802261506
- Jocher, A., Bonnety, J., Gomez, T., Pitsch, H., and Legros, G. (2019). Magnetic control of flame stability: Application to oxygen-enriched and carbon dioxide-diluted sooting flames. *Proc. Combust. Inst.* 37, 5637–5644. doi:10.1016/j.proci.2018.05.156

funding acquisition; JD: investigation, data curation, and visualization; DL: supervision, project administration, and funding acquisition.

Funding

This work is supported by the Natural Science Foundation of Jiangsu Province (BK20200490), the National Natural Science Foundation of China (52106160, 52076110), and the Fundamental Research Funds for the Central Universities (30920031103).

Conflict of interest

The authors declare that the research was conducted in the absence of any commercial or financial relationships that could be construed as a potential conflict of interest.

Publisher's note

All claims expressed in this article are solely those of the authors and do not necessarily represent those of their affiliated organizations, or those of the publisher, the editors and the reviewers. Any product that may be evaluated in this article, or claim that may be made by its manufacturer, is not guaranteed or endorsed by the publisher.

Supplementary material

The Supplementary Material for this article can be found online at: <https://www.frontiersin.org/articles/10.3389/fenrg.2022.982391/full#supplementary-material>

- Joher, A., Bonnet, J., Pitsch, H., Gomez, T., and Legros, G. (2017). Dual magnetic effects on soot production in partially premixed flames. *Proc. Combust. Inst.* 36, 1377–1385. doi:10.1016/j.proci.2016.05.017
- Joher, A., Pitsch, H., Gomez, T., and Legros, G. (2015). Modification of sooting tendency by magnetic effects. *Proc. Combust. Inst.* 35, 889–895. doi:10.1016/j.proci.2014.05.139
- Kumar, M., Agarwal, S., Kumar, V., Khan, G. S., and Shakher, C. (2015). Experimental investigation on butane diffusion flames under the influence of magnetic field by using digital speckle pattern interferometry. *Appl. Opt.* 54, 2450–2460. doi:10.1364/ao.54.002450
- Li, J., Lai, S., Chen, D., Wu, R., Kobayashi, N., Deng, L., et al. (2021). A review on combustion characteristics of ammonia as a carbon-free fuel. *Front. Energy Res.* 9, 760356. doi:10.3389/fenrg.2021.760356
- Mehmood, K., Saifullah, M. I., and Abrar, M. M. (2020). Can exposure to PM_{2.5} particles increase the incidence of coronavirus disease 2019 (COVID-19)? *Sci. Total Environ.* 741, 140441. doi:10.1016/j.scitotenv.2020.140441
- Shinoda, M., Yamada, E., Kajimoto, T., Yamashita, H., and Kitagawa, K. (2005). Mechanism of magnetic field effect on OH density distribution in a methane-air premixed jet flame. *Proc. Combust. Inst.* 30, 277–284. doi:10.1016/j.proci.2004.07.006
- Takashi, A. (1990). A magnetically induced anomalous ring flame and quenching characteristics of butane flame. *Jpn. J. Appl. Phys.* 29, 864–867.
- Wang, Y., and Chung, S. H. (2019). soot formation in laminar counterflow flames. *Prog. Energy Combust. Sci.* 74, 152–238. doi:10.1016/j.pecs.2019.05.003
- Yamada, E., Kitagawa, K., Shinoda, M., and Yamashita, H. (2003b). Influence of four kinds of gradient magnetic fields on hydrogen-oxygen flame. *AIAA J.* 41, 1535–1541. doi:10.2514/2.2104
- Yamada, E., Shinoda, M., Yamashita, H., and Kitagawa, K. (2003a). Experimental and numerical analyses of magnetic effect on OH radical distribution in a hydrogen-oxygen diffusion flame. *Combust. Flame* 135, 365–379. doi:10.1016/j.combustflame.2003.08.005
- Yamada, E., Shinoda, M., Yamashita, H., and Kitagawa, K. (2002). Numerical analysis of a hydrogen-oxygen diffusion flame in vertical or horizontal gradient of magnetic field. *Combust. Sci. Technol.* 174, 149–164. doi:10.1080/713713079
- Ying, Y., and Liu, D. (2017). Effects of butanol isomers additions on soot nanostructure and reactivity in normal and inverse ethylene diffusion flames. *Fuel* 205, 109–129. doi:10.1016/j.fuel.2017.05.064
- Ying, Y., and Liu, D. (2018). Nanostructure evolution and reactivity of nascent soot from inverse diffusion flames in CO₂, N₂, and He atmospheres. *Carbon* 139, 172–180. doi:10.1016/j.carbon.2018.06.047
- Ying, Y., and Liu, D. (2021). Soot properties in ethylene inverse diffusion flames blended with different carbon chain length Alcohols. *Fuel* 287, 119520. doi:10.1016/j.fuel.2020.119520
- Ying, Y., Xu, C., Liu, D., Jiang, B., Wang, P., and Wang, W. (2017). Nanostructure and oxidation reactivity of nascent soot particles in ethylene/pentanol flames. *Energies* 10, 122. doi:10.3390/en10010122